SI. Table 1. Autogrid parameters

	hMD-2/lipid IV_A	mMD-2/lipid IV_A
Grid box	76x126x86	94x126x104
Spacing	0.2083	0.225
Grid center	-2.574, 16.526, 17.163	-27.344, -16.643, 15.687
smooth	0.5	0.5
dielectric	-0.1465	-0.1465
Torsions	IV_A 6 torsions	IV_A 30 torsions

SI Figure legend:

SI Figure 1. Monomeric MD-2 of human or mouse origins can be purified into homogeneity. High 5 cells were infected by baculoviruses encoding hMD-2 (left) or mMD-2 (right) with a C-terminal protein A tag, at the multiplicity of infection of 2. After 3 days of infection, supernatants (lane 1) were separated from the cells, clarified by centrifugation and filtration, and then loaded onto an IgG affinity column. Elution fractions (lanes 2, 3) were concentrated and subjected to size exclusion separation on a superdex 200 column (lanes 4-9). Lanes 8 and 9 demonstrate monomeric MD-2/protein A after the final gel filtration step, the fractions that are used in the subsequent functional assays. Note: double arrows indicate the position of monomeric MD-2 with the protein A tag. Heterogeneity arises from glycosylations. All samples were run on an 8-16% SDS-PAGE under non-reducing conditions. Lanes 1-3 were stained with Coomassie blue, and lanes 4-9 were silver stained.

SI Figure 2. Lipid IV_A is an LPS-antagonist in HEK293/hTLR4^{YFP} cells. HEK293/hTLR4^{YFP} cells were plated at a density of 20,000/well in 96 well dishes. The next day, cells were transfected with NF-κB-luciferase (40 ng/well) and renilla-luciferase (40 ng/well) reporter plasmids. After overnight transfection, supernatants were removed, cells were washed twice with PBS, and replenished with complete DMEM without serum supplements. Purified monomeric hMD-2 was added to all wells to a final concentration of 200 ng/ml (6.7 nM), and synthetic Eritoran or lipid IV_A was added to selected wells to a final concentration of 1 μg/ml. After 1 h of incubation, LPS was added to selected wells. Luciferase activity was measured in cell lysates the next day. Data are reported as mean + SD of three independent wells for each data point. The luciferase activities were normalized using renilla-luciferase. One representative dataset from 3 replicates is shown in the figure.

SI Figure 3. Flow cytometry analysis of mTLR4 surface expression. HEK293/mTLR4^{YFP} cells, HEK293 cells, immortalized wild type macrophages, and immortalized TLR4-deficient macrophages (1), were incubated for 15 min on ice with FcR blocking reagent (Macs) at 10 μg/ml in blocking buffer (1% BSA in PBS). Cells were then stained for 30 min with sa1521 (black line), or control rat IgG (grey line), both directly conjugated with Alexa647, at the final concentration of at 5 μg/ml. After 3 times of washing with blocking buffer (1% BSA in PBS), cells were subject to flow cytometry analysis using a LSR 2 cytofluorimeter (BD Biosciences, San Jose, CA). 30,000 total events were acquired for each sample.

SI Figure 4. The docked hMD-2/lipid IV_A complex is essentially identical to the hMD-2/lipid IV_A co-crystal structure. The crystal structure of hMD-2 alone (PDB ID: 2E56) was

used to dock lipid IV_A (subtracted from PDB ID: 2E59) (1). The docked hMD-2/lipid IV_A was then overlaid to the co-crystal structure on hMD-2 sequences. Two perpendicular views are shown in the figure. Color scheme: red, hMD-2 in the co-crystal structure; yellow, lipid IV_A in the co-crystal structure; blue, hMD-2 in the docked complex; cyan, lipid IV_A in the docked complex.

SI Figure 5. The docked mTLR4/mMD-2/lipid IV_A complex is similar to the monomeric hTLR4/hMD-2/LPS complex isolated from the co-crystal structure (2). The mTLR4/mMD-2/lipid IV_A is overlaid to the monomeric hTLR4/hMD-2/LPS co-crystal structure on TLR4 sequences in (a). A zoomed-in view near the MD-2 pocket entrance is shown in (b). Color scheme: hTLR4 (purple ribbon), hMD-2 (pink ribbon), LPS in the human complex (cyan sticks and lines); mTLR4 (white ribbon), mMD-2 (green ribbon), lipid IV_A in the mouse complex (yellow sticks). The lipid A part of LPS is shown as cyan sticks, and the core-polysaccharide of LPS is shown as cyan lines.

SI Figure 6. Ionic interactions between lipid IV_A and mTLR4 at the dimerization interface are essential for lipid IV_A responsiveness. HEK293 cells were transiently transfected with one of the mTLR4 mutant constructs and the reporter constructs. After overnight transfection, cells were stimulated with indicated concentrations of LPS (a) /lipid IV_A (b) and mMD-2 (200 ng/ml) under serum free conditions. The concentrations of LPS (a) /lipid IV_A (b) used in the assay were: 1000, 100, 10, and 0, ng/ml. Luciferase activity was measured in cell lysates the next day. One representative dataset from 4 replicates is shown in the figure. Data are reported as the mean + SD of three independent wells for each data point. Luciferase activities were normalized from renilla-luciferase activity.

SI Figure 7. Human TLR4 gained lipid IV_A responsiveness when positive charges from mTLR4 were grafted onto hTLR4 at the dimerization interface in the presence of mMD-2. HEK293 cells were transiently transfected with one of the hTLR4 mutant constructs and reporter constructs. After overnight transfection, cells were stimulated with indicated concentrations of LPS/lipid IV_A and mMD-2 (200 ng/ml) under serum free conditions. The concentrations of LPS (a) /lipid IV_A (b) used in the assay were: 1000, 100, 10, and 0, ng/ml. Luciferase activity was measured in cell lysates the next day. One representative dataset from 4 replicates is shown in the figure. Data are reported as the mean + SD of three independent wells for each data point. Luciferase activities were normalized from renilla-luciferase activity.

SI Figure 8. Mouse MD-2 differs from human MD-2 in the hydrophobic pockets and adjacent surface charges. The electrostatic surface charges were calculated for hMD-2 (left) and mMD-2 (right) in MolMol (3). Residues that differ between hMD-2 and mMD-2 are labeled. The hydrophobic pockets (solid black arrows) and dimerization interface (dashed circles) are labeled. Red for negatively charged surface, blue for positively charged surface, and white for non-charged surface.

SI Reference:

1. Ohto, U., Fukase, K., Miyake, K., and Satow, Y. (2007) *Science* **316**, 1632-1634
2. Park, B. S., Song, D. H., Kim, H. M., Choi, B. S., Lee, H., and Lee, J. O. (2009) *Nature*
3. Koradi, R., Billeter, M., and Wuthrich, K. (1996) *J Mol Graph* **14**, 51-55, 29-32

Meng et al., SI Figure 1

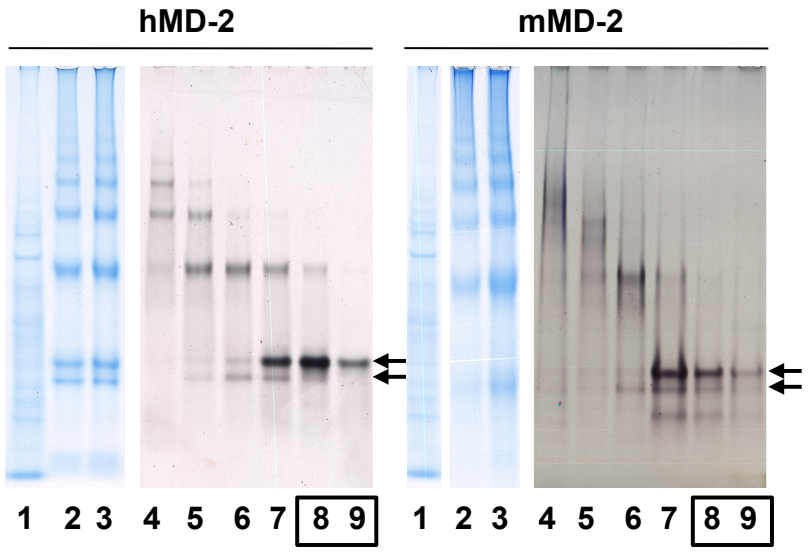

Meng et al., SI Figure 2

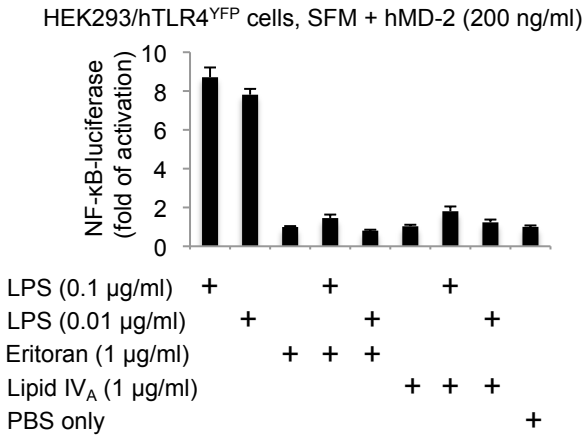

Meng et al., SI Figure 3

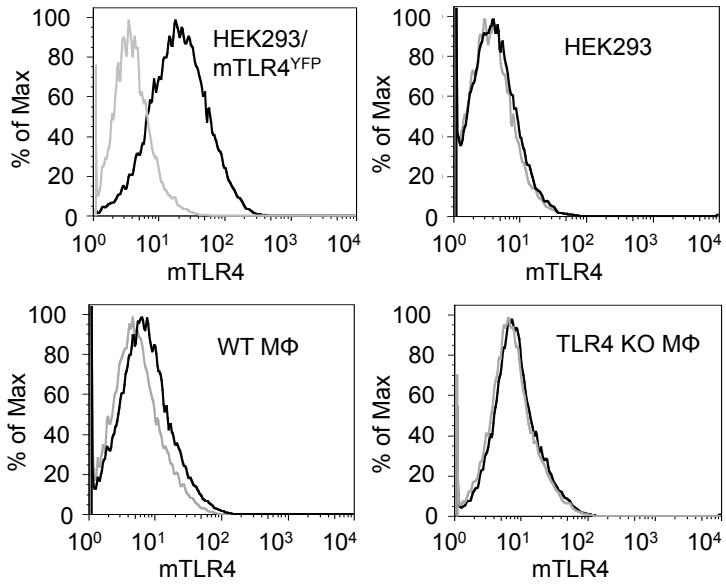

Meng et al., SI Figure 4

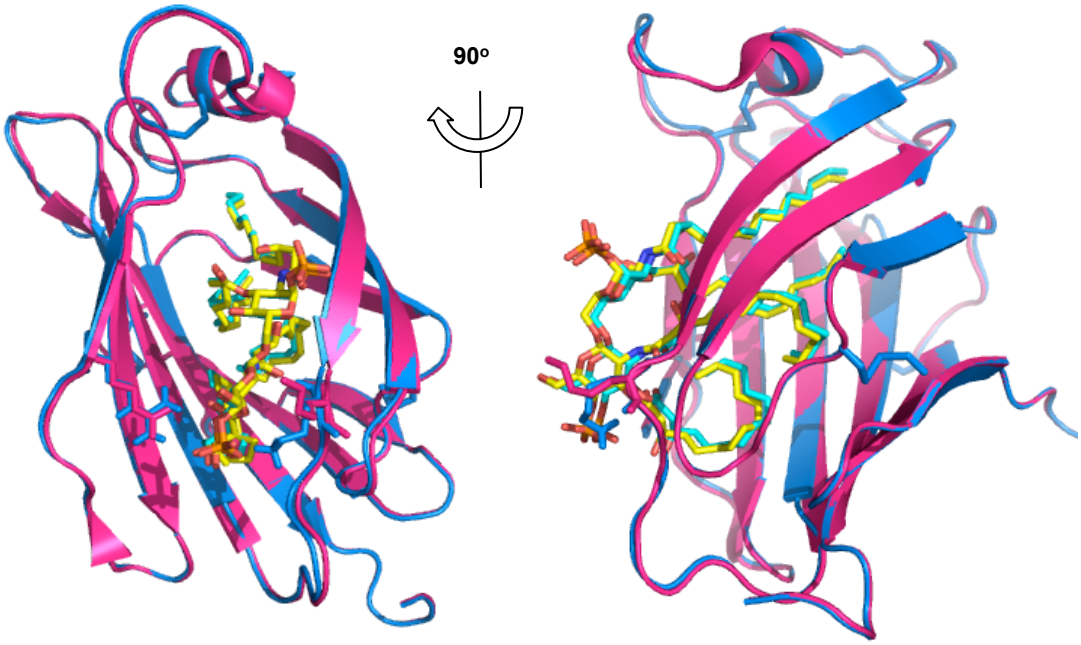

Meng et al., SI Figure 5

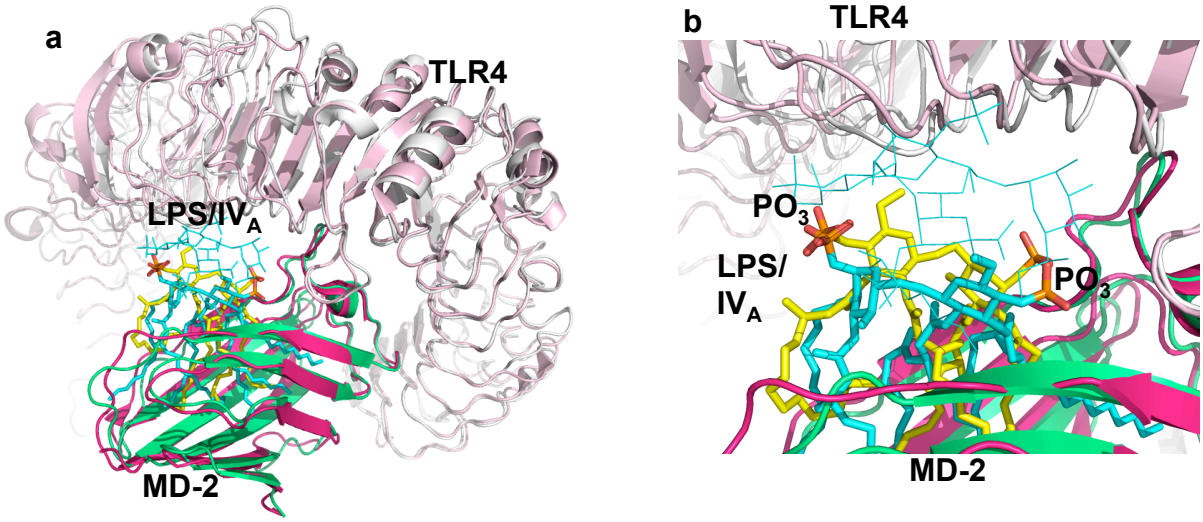

Meng et al., SI Figure 6

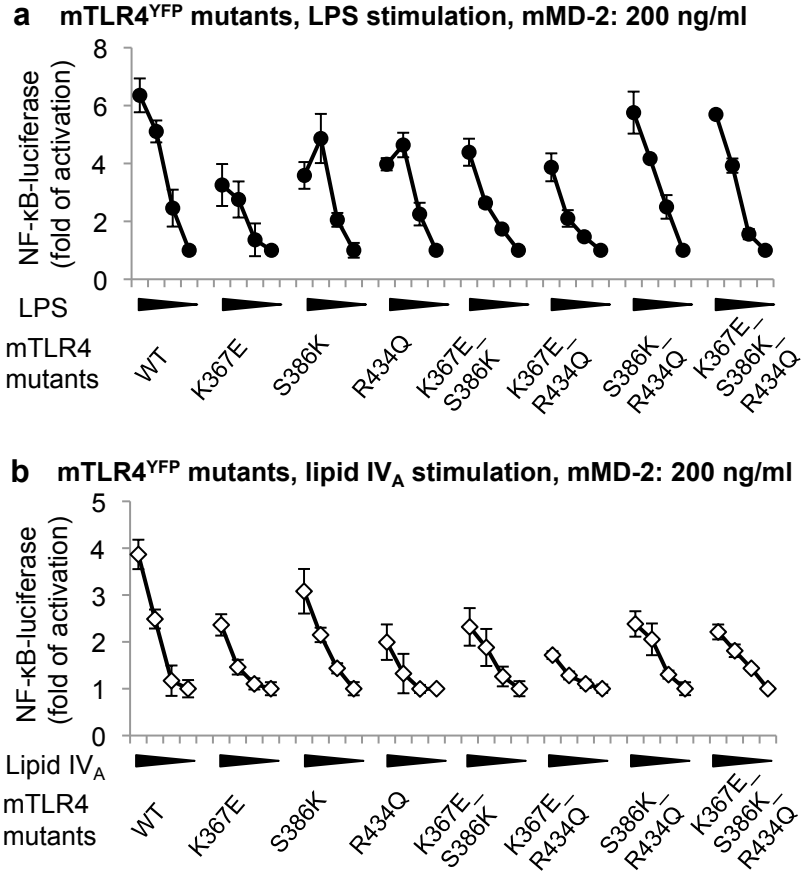

Meng et al., SI Figure 7

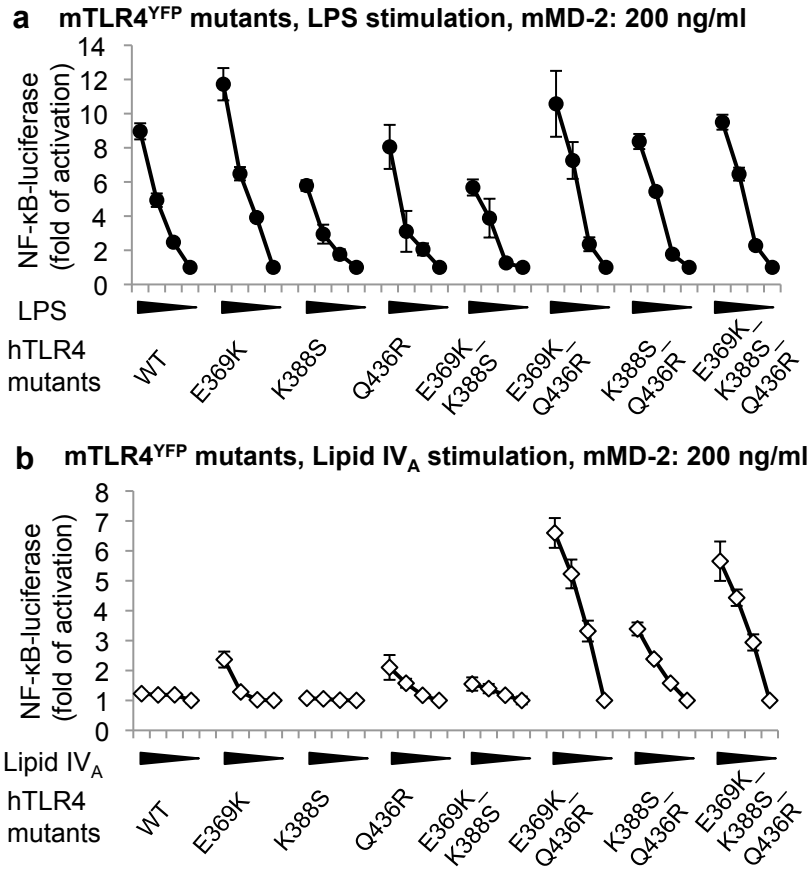

Meng et al., SI Figure 8